

COMPUTATIONAL PHYSICS

The Computational Physics Section publishes articles that help students and their instructors learn about the physics and the computational tools used in contemporary research. Most articles will be solicited, but interested authors should email a proposal to the editors of the Section, Jan Tobochnik (jant@kzoo.edu) or Harvey Gould (hgould@clarku.edu). Summarize the physics and the algorithm you wish to include in your submission and how the material would be accessible to advanced undergraduates or beginning graduate students.

Stability of planetary systems: A numerical didactic approach

Renato Pakter^{a)} and Yan Levin^{b)}

Instituto de Física, UFRGS, Caixa Postal 15051, CEP 91501-970 Porto Alegre, Rio Grande do Sul, Brazil

(Received 24 October 2018; accepted 24 October 2018)

We discuss the numerical methods needed to study the dynamics of interacting planetary systems. We argue that the most appropriate method for studying the many-body dynamics is Runge-Kutta with an adaptive step size. We demonstrate that planetary systems are highly susceptible to catastrophic events in which collisions between the planets are almost unavoidable. We then discuss a recently proposed mechanism that explains how planetary systems may have spontaneously evolved into a self-organized periodic state in which catastrophic events are avoided.

© 2019 American Association of Physics Teachers.

<https://doi.org/10.1119/1.5079541>

I. INTRODUCTION

The stability of the solar system has been a topic of debate since the birth of modern physics. After introducing his law of Universal Gravitation, Newton realized that small gravitational interactions between planets could result in the perturbation of their orbits that over time might lead to catastrophic events, such as collisions or expulsions of planets from the solar system.¹ To overcome this problem Newton appealed to divine intervention in which God would periodically adjust the orbits to prevent catastrophes. Leibnitz, Newton's contemporary, opposed this theological solution,² and argued that Gods should be able to choose stable orbits *a priori*. The debate about the stability of the solar system has provided much impetus to the development of classical mechanics.³ In spite of this effort over the centuries, the stability of planetary systems can be proven rigorously only for unrealistically small planetary masses of 10^{-320} of the solar mass.⁴ Therefore, we are forced to use numerical methods to consider realistic planetary masses.

The use of numerical methods has become a fundamental ingredient of the toolkit of contemporary physicists. The percentage of physical problems that can be solved analytically is progressively decreasing with time, and numerical methods have become unavoidable. A common example is the necessity to solve differential equations. In the present paper, we will discuss numerical methods for studying initial value problems appropriate to the exploration of planetary dynamics.

II. NUMERICALLY SOLVING A GRAVITATIONAL PROBLEM

We start by considering the gravitational interaction between two point particles of mass m . Without loss of generality we assume that the particle motion is restricted to the

x - y plane. From Newton's second law and law of gravitation, we obtain that the trajectories of particles satisfy

$$m \frac{d^2 \vec{r}_1}{dt^2} = \vec{F}_1(\vec{r}_1, \vec{r}_2) = \frac{-Gm^2(\vec{r}_1 - \vec{r}_2)}{r_{12}^3}, \quad (1)$$

$$m \frac{d^2 \vec{r}_2}{dt^2} = \vec{F}_2(\vec{r}_1, \vec{r}_2) = \frac{-Gm^2(\vec{r}_2 - \vec{r}_1)}{r_{12}^3}, \quad (2)$$

where $\vec{r}_i = x_i \hat{e}_x + y_i \hat{e}_y$ are the position vectors of each particle with $i = 1, 2$, $r_{12} = \sqrt{(x_1 - x_2)^2 + (y_1 - y_2)^2}$ is the distance between the particles, $\vec{F}_1(\vec{r}_1, \vec{r}_2)$ and $\vec{F}_2(\vec{r}_1, \vec{r}_2)$ are the forces acting on them, and $G = 6.67 \times 10^{-11} \text{ m}^3/\text{kg s}^2$ is the gravitational constant. Because the interaction is two-body, we could, in principle, find an exact, analytical solution for the particles' evolution. However, such a solution is not the aim here. Instead, we want to investigate the problem from a numerical perspective to gain insights into the features of numerical techniques.

Numerical methods for integrating ordinary differential equations typically consider first-order equations. We can straightforwardly express Eqs. (1) and (2) in terms of first-order differential equations by defining the particle velocities $\vec{v}_i = v_{xi} \hat{e}_x + v_{yi} \hat{e}_y$, such that

$$\frac{d\vec{r}_i}{dt} = \vec{v}_i, \quad (3)$$

$$\frac{d\vec{v}_i}{dt} = \frac{\vec{F}_i(\vec{r}_1, \vec{r}_2)}{m}. \quad (4)$$

Numerical methods to solve ordinary differential equations generally consist in approximating the continuous time evolution by a conveniently constructed time discretized version. The discretized version is usually called a map because

it maps the values of the variables at time t onto their values at time $t + \Delta t$, where Δt is the time step. An intuitive method to construct such map is to directly substitute the time derivative, $dx/dt = v_x(t)$ by a finite difference $\Delta x/\Delta t = [x(t + \Delta t) - x(t)]/\Delta t = v_x(t)$. By isolating $x(t + \Delta t)$, we readily obtain the map $x(t + \Delta t) = x(t) + v_x(t)\Delta t$. This approach leads to the Euler method. We apply it to Eqs. (3) and (4) and obtain

$$\vec{r}_i(t + \Delta t) = \vec{r}_i(t) + \vec{v}_i(t)\Delta t, \quad (5)$$

$$\vec{v}_i(t + \Delta t) = \vec{v}_i(t) + \frac{\vec{F}_i(\vec{r}_1(t), \vec{r}_2(t))}{m} \Delta t. \quad (6)$$

We expect that if Δt is sufficiently small, the trajectory obtained from Eqs. (5) and (6) will accurately describe the evolution given in Eqs. (1) and (2). However, if Δt is too small, that number of calculations needed will increase making the computation more demanding.

The Euler method is first order because its accuracy per step scales linearly with Δt . Higher order methods whose accuracy per step scale as $(\Delta t)^n$, where n is the order of the method, can also be constructed. A widely used example is the Runge-Kutta method,⁵ which can be extended to any order. In particular, the Euler method corresponds to first-order Runge-Kutta.

To test the results obtained from the application of Eqs. (5) and (6) to describe the system evolution, let us consider an example. For simplicity, we assume that the masses are $m = 1.5 \times 10^{10}$ kg, so that $Gm = 1.0 \text{ m}^3 \text{ s}^{-2}$. The particles are initially located at $x_1 = -10 \text{ m}$, $y_1 = -0.5 \text{ m}$, $x_2 = 10 \text{ m}$, $y_2 = 0.5 \text{ m}$ and move toward one another with initial velocities $v_{x1} = 1.0 \text{ m/s}$, $v_{x2} = -1.0 \text{ m/s}$, and $v_{y1} = v_{y2} = 0$. The trajectories obtained using Eqs. (5) and (6) with $\Delta t = 0.1 \text{ s}$ (thick curves) and $\Delta t = 0.5 \text{ s}$ (thin curves) are shown in Fig. 1. We see that for both values of Δt the particles initially interact very weakly, moving in nearly straight lines toward one another. As they become closer, they are scattered, quickly changing their propagation direction. However, the scattered angles are different for $\Delta t = 0.1 \text{ s}$ and $\Delta t = 0.5 \text{ s}$.

We expect that the $\Delta t = 0.1 \text{ s}$ case is more likely to be correct. To test this assumption, we recall that the total energy of the system

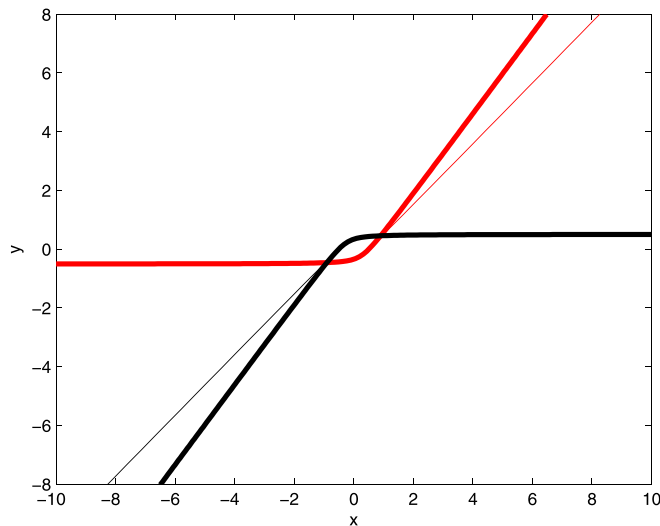


Fig. 1. Trajectories obtained numerically using Eqs. (5) and (6) for the scattering of two particle masses. The thick curve corresponds to the time step $\Delta t = 0.1 \text{ s}$, and the thin curve corresponds to $\Delta t = 0.5 \text{ s}$.

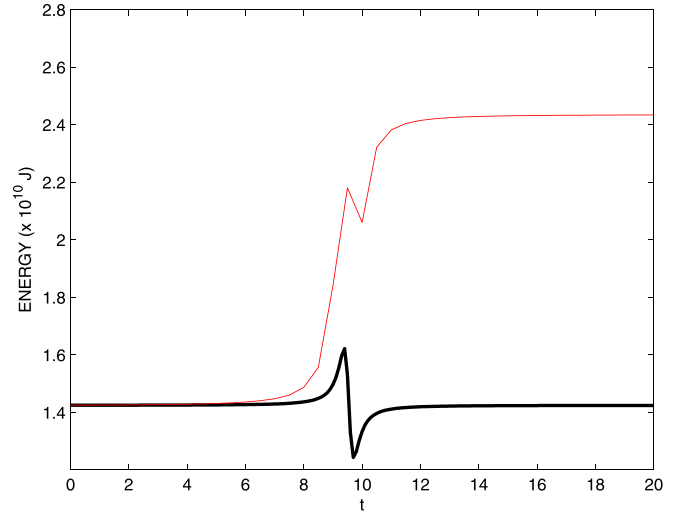


Fig. 2. The total energy as a function of time for the scattering of two point masses. The thick black curve corresponds to $\Delta t = 0.1 \text{ s}$, and the thin (red) curve to $\Delta t = 0.5 \text{ s}$.

$$E = \frac{mv_1^2}{2} + \frac{mv_2^2}{2} - \frac{Gm^2}{r_{12}} \quad (7)$$

is a conserved quantity of the motion. The energies as a function of time for $\Delta t = 0.1 \text{ s}$ and $\Delta t = 0.5 \text{ s}$ are shown in Fig. 2. We see that in both cases the energy changes near the scattering point (around $t = 10 \text{ s}$). Clearly, the energy variations and numerical errors are much more pronounced for the larger Δt case, where the final energy is 70% higher than the initial energy.

We further explore conservation of energy to investigate other values of Δt in Fig. 3, where we plot the relative error $|E_{\text{final}} - E_{\text{initial}}|/E_{\text{initial}}$ as a function of Δt . Note that for $\Delta t > 0.2 \text{ s}$ the error starts not only to increase, but also has large oscillations with the variation of the time step. This oscillation indicates that the map obtained from Eqs. (5) and (6) for such high values of Δt is chaotic,⁶ and therefore does not properly describe the evolution. In contrast, for small

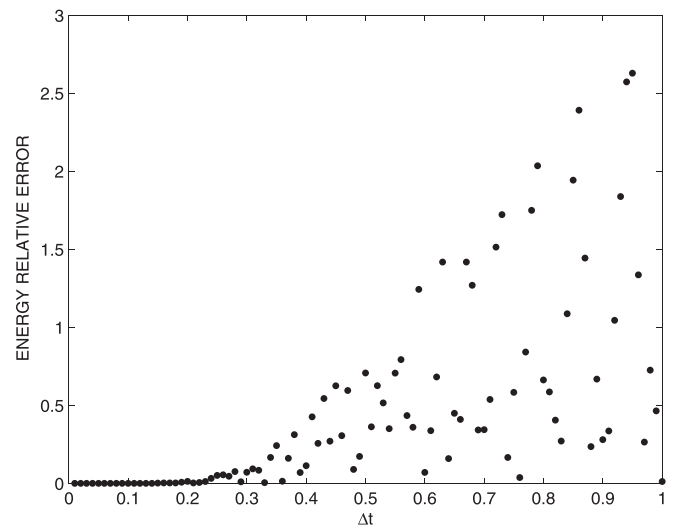


Fig. 3. The relative error of the energy, $|E_{\text{final}} - E_{\text{initial}}|/E_{\text{initial}}$, as a function of the time step Δt .

time steps ($\Delta t < 0.2$ s) the error decreases and a better system description is achieved with the Euler method.

From the construction of the Euler method, Eqs. (5) and (6), it appears that the smaller the time step, the more accurate the calculated trajectory. In particular, in the limit $\Delta t \rightarrow 0$ we expect the method to become exact. Indeed, this expectation would be the case if the numerical calculations were performed with numbers of infinite precision. However, the computer stores numbers using a finite number of digits and truncates (or rounds off) numbers after each mathematical operation. This truncation also generates numerical errors. This type of error increases with the number of truncations/operations performed. The truncation error is larger when the time step is smaller, which requires a large number of calculations.

We compute the relative error of the energy for a wide range of values of Δt and plot the results on a log-log scale in Fig. 4. We see that the relative error is a non-monotonic function of Δt and increases if the time step becomes too small. In particular, Fig. 4 shows an optimal time step that leads to a very small energy variation, $\Delta t = 10^{-3}$ s. The optimum value is expected to change if we modify the initial conditions, the values of the masses, the number of particles in the system, and the force. Moreover, in many systems there are no conserved quantities that could be used to determine the optimal time step.

How can we generally find the optimal time step to guarantee the accuracy of our numerical results? One idea is to use two integration methods of different accuracies, for example, of different orders. We then consider the result obtained with the higher accuracy method as the gold standard. When the lower accuracy result matches the gold standard to the desired tolerance as the time step is varied, the given time step is taken. Usually, the comparison between the two methods is done directly at the variables level by computing, for instance, the Euclidean distance in phase space between the two numerical solutions. In this way there is no need for a known conserved quantity. In practice, this procedure can be continuously used along the integration to determine an optimal Δt for each part of the evolution, thus, adapting the time step to satisfy the tolerance requirements and to speed up the simulation.⁵ A numerical subroutine

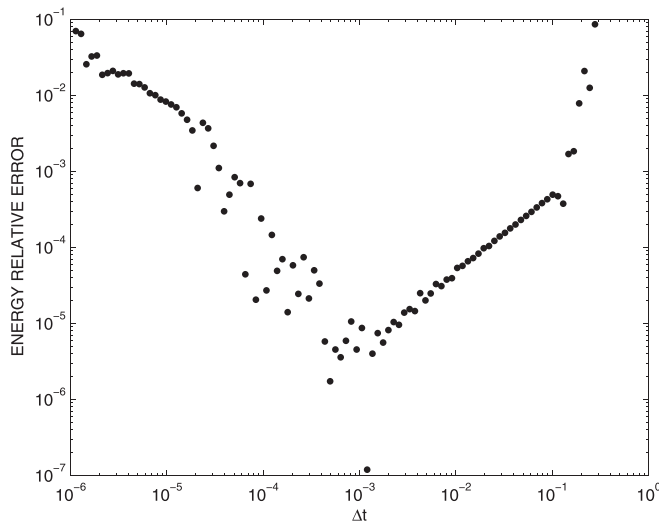


Fig. 4. The relative error of the energy, $|E_{\text{final}} - E_{\text{initial}}|/E_{\text{initial}}$, as a function of the time step Δt .

called *dverk* which implements the Runge-Kutta algorithm with an adaptive step size is available from the public repository Netlib.⁷

III. STABILITY OF PLANETARY SYSTEMS

We employ an adaptive time step algorithm that uses embedded fifth order and sixth order Runge-Kutta estimates to compute the solution with a tolerance of 10^{-10} to investigate the planetary dynamics. The system consists of N planets interacting gravitationally with each other and with a star. The dynamics of the i th body in the planetary system is given by

$$m_i \frac{d^2 \vec{r}_i}{dt^2} = - \sum_{j \neq i} \frac{G m_i m_j (\vec{r}_i - \vec{r}_j)}{r_{ij}^3}, \quad (8)$$

where $i, j = 1, \dots, N+1$, with the $i = N+1$ corresponding to the star. To simplify the calculations, we assume that the motion is confined to the x - y plane, and that all the planets have the same mass m and the star mass is M , with $M \gg m$.

Because there are more than two bodies in the system, the dynamics may become chaotic.⁶ Chaos can be detrimental to the stability of a planetary system and can result in catastrophic events. Because the gravitational potential is bounded from above and is unbounded from below, chaos can lead some planets to either gain enough kinetic energy to escape altogether from the planetary system, or to lose kinetic energy and end up falling into the star or to collide with another planet. These catastrophic events are what we found by numerically integrating Eq. (8) for arbitrary initial conditions. For example, we consider a system with a star of mass $M = 2.0 \times 10^{30}$ kg (the mass of our sun) and $N = 8$ planets with mass $m = 0.0001 M$ (one tenth of the mass of Jupiter) with radii initially uniformly distributed between 2 and 16 a.u. (the *astronomical unit* corresponds to the mean earth-sun distance). The initial velocity of each planet is chosen such that in the absence of its gravitational interaction with the other planets, it would follow a stable circular orbit around the star.

The planets and the star can collide with each other during the evolution, leading to the termination of the simulation. To prevent such catastrophic events, we introduced a softening of the gravitational potential.⁸ The softened potential is constructed so that the force between the masses vanishes for separations $r = 0$ and the interaction potential and its derivative are continuous at the cutoff distance $r = d$, comparable to the planetary diameter

$$V(r) = \begin{cases} -\frac{(2d^3 - 2dr^2 + r^3)Gm^2}{d^4} & (r \leq d) \\ -\frac{Gm^2}{r} & (r > d). \end{cases} \quad (9)$$

In our simulations, we used d on the order of 10^{-3} a.u.

In Fig. 5, we show the planetary orbits obtained for the first two thousand earth-years of the evolution. We see that the orbits are nearly circular around the sun, and there is just a small precession of the orbits due to the gravitational interaction between the planets. In Fig. 6, we show the evolution of the distance between each planet and the star. In Fig. 6(a) we show the evolution up to $t = 20$ thousand earth-years. Notice that up to $t = 6$ thousand earth-years the planets

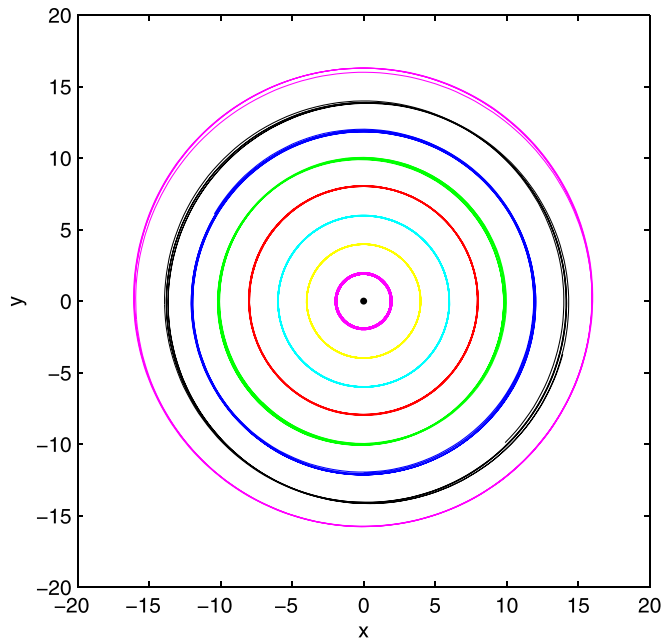


Fig. 5. Planetary orbits found at the initial stage of the planetary evolution up to $t =$ two thousand earth-years. The distances are measured in astronomical units (a.u.).

maintain their nearly circular orbits around the star with some minor radial oscillations. After this time, the planets start to show erratic trajectories and even change their order with respect to the star. For instance, if we consider the planet that starts at 14 a.u. from the star (black curve in Fig. 6), we see that from $t \approx 8$ to 10 thousand earth-years it switches places with the planet that started at 16 a.u., becoming the outermost planet. Moreover, as times evolves, this same planet undergoes other jumps, becoming the fourth closest planet at $t = 20$ thousand earth-years. The jumps occur when two bodies pass near each other causing a sudden change in momentum analogous to the slingshot effect used to accelerate artificial satellites.

As the system evolves even further, slingshot type events drive the planets to very large radial velocities that allow them to escape the planetary system. See Fig. 6(b) where we show the evolution for longer times in a log-log plot. Half of the planets are gone by $t = 1$ million earth years, the duration of the simulation. We stress that the type of phenomena seen in Fig. 6 occurs for almost any initial condition—it is almost

impossible to find at random an initial condition that leads to a stable, durable, planetary system. We note that because we are using the adaptive time step numerical method with a stringent tolerance, the catastrophic events are real and are not induced by the numerical errors. This observation can be verified, for instance, by computing conserved dynamical quantities such as the total energy of the system

$$E = \sum_{i=1}^N \left[\frac{m_i v_i^2}{2} - \frac{1}{2} \sum_{j \neq i} \frac{G m_i m_j}{r_{ij}} \right], \quad (10)$$

and the total angular momentum

$$L = \sum_{i=1}^N m_i (x_i v_{yi} - y_i v_{xi}). \quad (11)$$

The evolution of these quantities is shown in Fig. 7, confirming that despite the very complex planetary dynamics, the energy and angular momentum are conserved to less than 0.01% during the entire evolution. Note that the total energy is negative, corresponding to a bound state, meaning that the modulus of the attractive gravitational potential energy is larger than the kinetic energy. Nevertheless, planets can escape from the system.

IV. CONCLUSIONS

To simulate the dynamics of a planetary system over a span of billions of years is not an easy task. The integration time step of such simulations cannot be too small, otherwise the simulations will result in a large roundoff error due to the finite precision of numbers stored in computer memory. We have argued that one practical way to overcome this difficulty is to use a Runge-Kutta algorithm with an adaptive step size. The advantage of this approach is that the integrator automatically adjusts the time step to capture the most relevant time scale of the system. By using this approach, we have demonstrated that even an extremely symmetrical, idealized, system of the planets in precise circular orbits around the star, becomes unstable over millennia due to small inter-planetary interactions. These gravitational interactions lead to catastrophic events in which planets can collide or be ejected from the planetary system. We observe that it is practically impossible to find initial conditions that lead to stable arrangements of the planets in the infinite time limit, unless

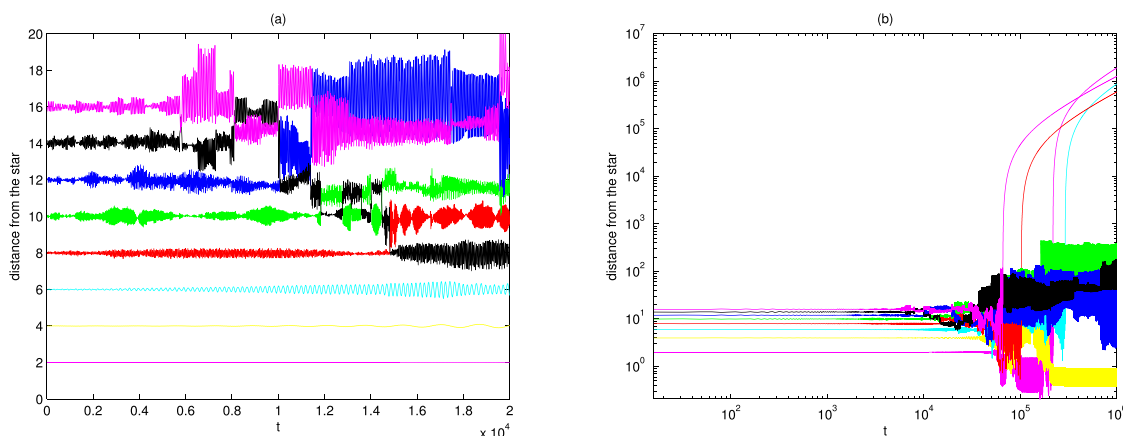


Fig. 6. Evolution of the distance of the planets from the star. The time is measured in earth-years and the distance in astronomical units.

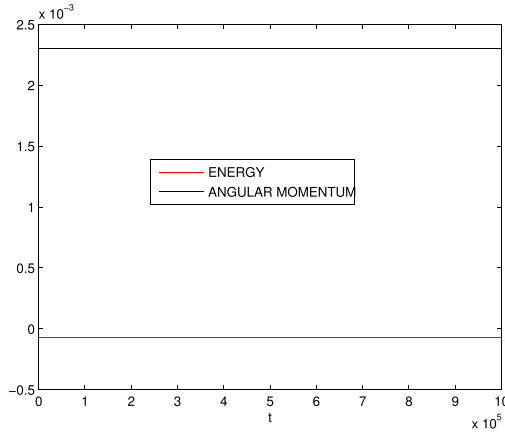


Fig. 7. Evolution of the total energy and total angular momentum of the planetary system. The time is measured in earth-years, energy in units of $GM^2/(2\pi)^2 R = 4.5 \times 10^{37}$ J, and angular momentum in units of $\sqrt{GM^3 R}/2\pi = 1.4 \times 10^{45}$ kg m²/s, where $R = 1$ a.u. = 1.5×10^{11} m.

the masses of the planets are unrealistically small, as was noted by Henon more than fifty years ago.⁴

What can then explain the stability of the solar system, which appears to be more or less unperturbed over the span of billions of years? In a recent paper,⁸ it was argued that the stability of planetary systems may be a consequence of energy non-conserving perturbations, such as the interaction of primordial planetesimals with a residual gas and dust of the protoplanetary disk. The dust particles of the protoplanetary disk move in Keplerian orbits with angular velocity $\omega(r) = \sqrt{GM}/r^3$, where r is the distance from the star.^{9,10} We can suppose that if the velocity of the planetesimal at a given position r is lower than that of the surrounding dust, it will gain kinetic energy from the collisions with the dust particles. In contrast, if the velocity is higher than the rotational velocity of the gas and dust particles, the planetesimal will lose energy. As time progresses the amount of gas and dust in the protoplanetary disk will be progressively depleted, and eventually the interaction of planets with the disk will become negligibly small. We find⁸ that this small viscous-like interaction drives a protoplanetary system into a periodic self-organized state in which the relative arrangement of planets repeats itself each synodic period T (see Problem 3). Note that the trajectory of the individual planets can be very complicated, with the orbits precessing around the star. Nevertheless, the relative arrangement of the planets repeats itself exactly each $t = T$. Once achieved, the periodic state will persist forever.

We stress that for realistic planetary systems it is practically impossible to find *a priori* initial conditions which will result in periodic orbits. Such initial conditions correspond to a set of measure zero of all possible initial conditions. Nevertheless, a non-energy conserving perturbation introduced in Ref. 8 turns such periodic orbits “attractive,” driving a planetary system toward a self-organized periodic state (see Problem 3). This may be a possible explanation for the surprising stability of the solar system and of other exoplanetary systems which appear to be quite abundant in the universe.

V. SUGGESTED PROBLEMS

- (1) Consider two planets of mass m , one located at $x_1 \rightarrow -\infty$, $y_1 = -b$ and moving with velocity $\vec{v} = v_0 \vec{e}_x$ and the other at $x_1 \rightarrow \infty$, $y_1 = +b$ and moving with velocity

$\vec{v} = -v_0 \vec{e}_x$. The trajectories of the planets are similar to Rutherford scattering, with the scattering angle given by $\theta = 2\arctan(Gm/4v_0^2 b)$. Use the subroutine *dverk* for Runge-Kutta with an adaptive step size available from Netlib⁷ to calculate the trajectories of the two planets and verify the Rutherford scattering formula.

- (2) Use the subroutine *dverk* to compute the orbits of four planets of mass $m = 0.001 M$, approximately equal to that of Jupiter, uniformly distributed from 1 to 4 a.u. along the x axis from a star of mass M equal to that of our sun. Choose the initial velocity of each planet such that in the absence of interactions with the other planets it would follow a circular orbit. How much time in earth years does it take before one of the planets escapes from the planetary system? To prevent numerical instability use the softened gravitational potential, Eq. (9) with the softening radius equal to that of Jupiter. Suggestion: rewrite the equations in dimensionless form with the time measured in earth years and the distance in a.u.
- (3) If a planet at position r_i rotates faster than the surrounding dust, it will lose energy to the dust and will slow down. If it rotates slower, it will gain energy from the collisions with dust particles and will speed up. Phenomenologically the interaction of planetesimals with a protoplanetary disk can be modeled as an effective force⁸

$$\vec{F}_i = -\beta(2\pi)^2(v_i^{\text{dust}} - v_i^\theta) \left[L - m \sum_i v_i^\theta r_i \right] \hat{e}_\theta, \quad (12)$$

where $\beta \approx 0.0025$ a.u.⁻² is a small phenomenological constant that controls the interaction between dust and planets, $v_i^{\text{dust}} = r_i \omega(r_i)$ is the angular velocity of dust at the location of planet i , and v_i^θ is the angular velocity of planet i

$$v_i^\theta = \frac{\dot{y}_i x_i - y_i \dot{x}_i}{r_i}. \quad (13)$$

The term in the square brackets of Eq. (12) is included so that the interaction between the dust and the planets “turns off” when the net total angular momentum reaches a predetermined value $L \approx 2\sqrt{GM^3 R}/\pi$. This form is used to model a progressive depletion of dust from the protoplanetary disk. Add the planet-dust interaction to the planetary system of Problem 2 and show that after a million earth years, the planetary system will reach a periodic state in which perihelion distance of the outermost planet is repeated each synodic period $T \approx 3.7$ years. Note that there is a synchronization between the planets with the ratio between all the orbital periods of different planets being a rational number. To simplify the analysis fix the position of the star at the origin during the simulation.

ACKNOWLEDGMENTS

This work was partially supported by the CNPq, the National Institute of Science and Technology Complex Fluids INCT-FCx, and by the US-AFOSR under the Grant No. FA9550-16-1-0280.

^a)Electronic mail: pakter@if.ufrgs.br

^b)Electronic mail: levin@if.ufrgs.br

- ¹I. Newton, *Opticks: Or, A Treatise of the Reflections, Refractions, Inflexions and Colours of Light*, 4th ed. (Dover, New York, 1730), republication of London 1730, printed for William and John Innys at the West End of St. Paul's.
 - ²G. S. Morson, *Narrative, Philosophy and Life* (Springer, Boston, 2014), p. 123.
 - ³J. Laskar, "Is the solar system stable?," *Chaos, Prog. Math. Phys.* **66**, 239–270 (2013).
 - ⁴J. Laskar, "Michel Henon and the stability of the solar system," e-print [arXiv:1411.4930](https://arxiv.org/abs/1411.4930).
 - ⁵W. H. Press, B. P. Flannery, S. A. Teukolsky, and W. T. Vetterling, *Numerical Recipes in C: The Art of Scientific Computing* (Cambridge U.P., Cambridge, 1988).
 - ⁶A. J. Lichtenberg and M. A. Lieberman, *Regular and Chaotic Dynamics*, 2nd ed. (Springer, New York, 1992).
 - ⁷The Netlib repository contains freely available software, documents, and databases of interest to the scientific computing communities, <www.netlib.org/>.
 - ⁸R. Pakter and Y. Levin, "Stability and self-organization of planetary systems," *Phys. Rev. E* **97**, 042221 (2018).
 - ⁹N. I. Shakura and R. A. Sunayev, "Black holes in binary systems. Observational appearance," *Astron. Astrophys.* **24**, 337–355 (1973).
 - ¹⁰D. Lynden-Bell and J. E. Pringle, "The evolution of viscous discs and the origin of the nebular variables," *MNRAS* **168**, 603–637 (1974).
-